Molecular Crystals and Liquid Crystals Science and Technology. Section A. Molecular Crystals and Liquid Crystals

Publication details, including instructions for authors and subscription information:
http://www.tandfonline.com/loi/gmcl19

Birefringence and Dispersion of Uniaxial Media

Hedi Mattoussi [a], Mohan Srinivasarao [a b], Philip G. Kaatz [a c] & Guy C. Berry [a]

[a] Carnegie Mellon University, Department of Chemistry, Pittsburgh, PA, U.S.A.

[b] Polymer Science & Eng. Dept., University of Massachusetts, Amherst, MA, 01003

[c] TEH- Honggerberg (HPF) Institut fur Quantenelektronik, Laboratorium fur Nichtlineare Optik, CH, 8093, Zurich

Version of record first published: 04 Oct 2006.

To cite this article: Hedi Mattoussi , Mohan Srinivasarao , Philip G. Kaatz & Guy C. Berry (1992): Birefringence and Dispersion of Uniaxial Media, Molecular Crystals and Liquid Crystals Science and Technology. Section A. Molecular Crystals and Liquid Crystals, 223:1, 69-84

To link to this article: http://dx.doi.org/10.1080/15421409208048241

Mol. Cryst. Liq. Cryst. 1992, Vol. 223, pp. 69–84
Reprints available directly from the publisher
Photocopying permitted by license only

Printed in the United States of America

BIREFRINGENCE AND DISPERSION OF UNIAXIAL MEDIA

HEDI MATTOUSSI, MOHAN SRINIVASARAO*, PHILIP G. KAATZ+, GUY C. BERRY
Carnegie Mellon University, Department of Chemistry, Pittsburgh, PA, U.S.A.

(Received October 10, 1991)

Abstract Refractive index measurements of uniaxial media (crystals and a polymer liquid crystal in the nematic phase) are described. The technique used, applicable for any anisotropic uniaxial medium, makes use of the birefringence to generate interference between the extraordinary and ordinary waves created after an incident plane polarized wave enters the crystal. The dispersion of the refractive indices for the uniaxial nematic polymer is discussed together with the implication it has on the third order nonlinear optic susceptibility measurements completed using the Third Harmonic Generation (THG) technique.

INTRODUCTION

The optical identification of uniaxial media (crystals and liquid crystals) requires measurements of two refractive indices; the ordinary, n_o, and extraordinary, n_e, defined, respectively, for a plane wave traveling in the medium with its wavevector parallel or perpendicular to the optic axis of the system.[1-3] Measurement of the nonlinear optical susceptibilities $\chi^{(i)}(i = 2, 3)$, using optical harmonics (second and third) generation, requires accurate knowledge of the refractive index n of the medium, and its dispersion $n = n(\omega)$ over a wide range of wavelengths, from UV-Visible to near infrared.[4-6] Therefore, accurate measurements of the refractive indices n_e, n_o, and their dispersion are needed for optical (linear and nonlinear) identification purposes of anisotropic uniaxial materials.

* Present address: Polymer Science & Eng. Dept.
University of Massachusetts
Amherst, MA 01003

+ Present address: ETH- Honggerberg (HPF)
Institut fur Quantenelektronik
Laboratorium fur Nichtlineare Optik
CH - 8093 Zurich

In this contribution, we present measurements of the refractive indices of uniaxial conventional crystals and a polymer liquid crystal. The method used involves transmission of polarized light and uses the birefringence of the medium to generate interference between the extraordinary and ordinary waves. In the first section we introduce the optics background and provide the analysis of the experimental method. This is followed by a brief description of the materials and the experimental arrangements we used. In the last section, a discussion of the data and its implications on other properties of uniaxial media is given.

EXPERIMENTAL SECTION

The general background and the mathematical formulation for the use of the birefringence of uniaxial media to generate and analyze the light interference are well known.[1,2] However, the methods we present here, namely the combination of the two procedures described below for measuring refractive indices and/or birefringence, are novel and offer an independent technique for refractive index measurements of uniaxial media. The wedge sample case has been used previously.[3]

Optics background

A plane polarized light wave incident on a uniaxial crystal may be decomposed into two secondary waves propagating with speeds c/n'' and c/n'; n'' and n' designate the extraordinary and ordinary refractive indices for waves traveling in the crystal at an average direction different from the principal optical directions of the medium, and c is the light speed in vacuum. These waves recombine at the exit with a light path difference δ (since $n'' \neq n'$) and interfere.[1,2] The experimental procedure used in the present study uses light interference between the extraordinary and ordinary waves propagating in the crystal, and subsequent analysis of the transmitted intensity is used to extract the individual refractive indices and/or the birefringence, depending on the extent of the data analysis. A polarizer (P) may be used to define the incident polarization and an analyzer (A) at an angle Ψ with respect to P is used to select the outgoing one. The optic axis $\underline{n}$ may be set at an angle Φ with respect to the polarizer P. A particularly simple case of this method, which is

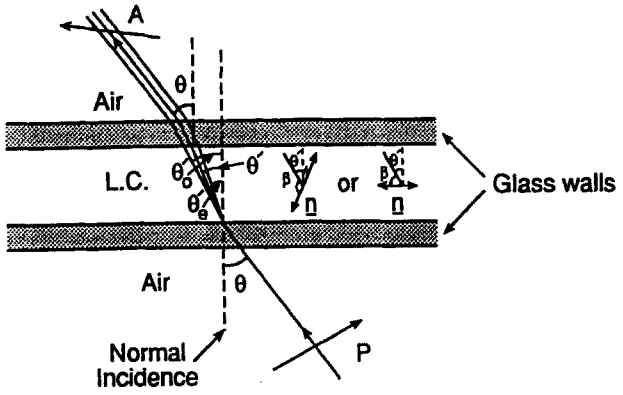

FIGURE 1 Extraordinary and ordinary light paths in a flat planar uniaxial medium

discussed below, correspond to $\psi = \pi/2$ (crossed polars) and the optic axis $\underline{n}$ laying in the plane of the sample, with ϕ such that $|\phi| = \pi/4$, as shown in Figs. 1 and 2. This allows an enhancement in the oscillation of the transmitted intensity I with δ, which is then given by:[1-3,9]

$$I_0 \sin^2\left(\frac{\pi\delta}{\lambda}\right) \qquad (1)$$

where I_0 is the amplitude of the transmitted intensity (I_0 depends on the transmission and reflection factors), and λ is the incident radiation wavelength.[1-3]

Because of the anisotropy of the medium, the extraordinary and ordinary waves created inside the crystal after a beam enters the medium with an incident angle θ have different refraction angles, θ_e' and θ_o', respectively. These waves travel with different light path lengths, d_e' and d_o', expressed as a function of the physical thickness of the sample d and the individual propagation angles in the medium θ_e' and θ_o': $d_e' = d/\cos\theta_e'$ and $d_o = d/\cos\theta_o'$. Since the birefringence is always small compared to the refractive indices ($|n_e - n_o| \ll n_e, n_o$), the refraction angles θ_e' and θ_o' may be approximated by an average value θ', and the following approximations can be used: $d_e' \simeq d_o' \simeq d' \equiv d/\cos\theta'$.[1-3] This allows one to derive analytical expressions for δ and the birefringence $n'' - n'$:[1-3,9]

$$\delta \simeq \frac{d\,(n'' - n')}{\cos\,\theta'} \qquad (2)$$

and

$$n'' - n' = (n_e - n_o) \sin^2 \beta \qquad (3)$$

where β is the angle between the direction of propagation of the light beam and the optic axis of the medium $\underline{n}$ (see Fig. 1). The refraction angle θ' obeys Snell's law: $\langle n_s \rangle \sin\theta' = n_{air} \sin\theta$, and the refractive index $\langle n_s \rangle$ for the "average" wave travelling in the crystal, is a function of β and ϕ:

$$\frac{1}{[\langle n_s(\phi,\beta)\rangle]^2} = \left[\frac{\sin^2\phi}{n_o^2} + \cos^2\phi \left[\frac{\sin^2\beta}{n_e^2} + \frac{\cos^2\beta}{n_o^2}\right]\right] \qquad (4)$$

where the angles θ' and β may be related trigonometrically.[1-3,9] For the particular cases where the rays are propagating in a plane either perpendicular or parallel to the optic axis $\underline{n}$, the relation between β and θ' becomes simple: $\beta = \pi/2$ and $\beta = \pi/2 - \theta'$, respectively. These cases correspond to the configurations where $\underline{n}$ is normal to and within the plane of incidence, respectively.[1-3,9] They are very useful, and they are simple cases. These cases, together with the conditions for the angle ϕ, will be referred to as follows: geometry 1 corresponds to $\beta = \pi/2$ and $\phi = \pi/4$, and geometry 2 corresponds to $\beta = \pi/2 - \theta'$ and $\phi = -\pi/4$, respectively. For the case where $\underline{n}$ is perpendicular to the plane of incidence (geometry 1), the expressions for δ and $\langle n_s \rangle$ (Eqs. (2) and (4)) may be simplified to:[9]

$$\delta \simeq \frac{d\,(n_e - n_o)}{\cos\theta'} \qquad (5)$$

and

$$\frac{1}{\langle n_s \rangle^2} = \frac{1}{2}\left[\frac{1}{n_e^2} + \frac{1}{n_o^2}\right] \qquad (6)$$

For the case where $\underline{n}$ is within the plane of incidence (geometry 2), δ and $\langle n_s \rangle$ become:

$$\delta \simeq d\,(n_e - n_o)\cos\theta' \qquad (7)$$

and

$$\frac{1}{\langle n_s(\theta')\rangle^2} = \frac{1}{2}\left[\frac{1}{n_o^2} + \left[\frac{\cos^2\theta'}{n_e^2} + \frac{\sin^2\theta'}{n_o^2}\right]\right] \qquad (8)$$

The use of the very same condition ($|n_e - n_o| \ll n_o, n_e$) may lead to a simple analytical solution for δ. In fact, within these

conditions, $\langle n_s \rangle$ can be approximated by the refractive index $\bar{n}$ of the average isotropic medium. The corresponding error committed using the approximation $\langle n_s(\theta') \rangle = \langle n_s \rangle = \bar{n}$ is small (about 5%) for uniaxial materials with relatively high birefringence; it is smaller when $|n_e - n_o|$ is modest.[9]

In what follows, we present two methods, deriving from the general formulation above, which describe different ways of varying the parameter δ, and hence of generating interference for the transmitted intensity. These methods pertain to monitoring δ as the physical light path in the crystal d' is varied. Subsequent analysis of the transmitted intensity is used to extract the refractive indices of the material.

Method 1: Translation of a wedge crystal

This method involves the use of a wedge sample where the variation of the physical thickness is monitored as the crystal is translated in the incident beam and within its plane.[3] At normal incidence, the two geometries introduced above become identical, and the mathematical formulation described above becomes very simple, since the refracted angles inside the crystal are kept fixed ($\theta_e' = \theta_o' = \theta' = 0$). This condition, together with those outlined above (optic axis within the plane and $|\phi| = \pi/4$), imply that the angle β is always fixed at $\pi/2$. The corresponding expression for δ is:

$$\delta \cong d(x)\ |n_e - n_o| \tag{9}$$

where x is the translational distance along the sample plane (see Fig. 2). The corresponding expression for d(x) reads as:

$$d(x) = d_o + x \tan \alpha \tag{10}$$

where d_o is an arbitrary length (thickness) depending on the initial point and α is the wedge angle of the sample. Therefore, δ becomes:

$$\delta \cong |n_e - n_o|\ (d_o + x \tan \alpha) \tag{11}$$

A scan of the intensity as a function of x will provide an oscillating function (Eq. 1). The minima locations obey the condition:

$$\delta_i \cong m_i \lambda \cong |n_e - n_o|\ (d_o + x_i \tan \alpha) \tag{12}$$

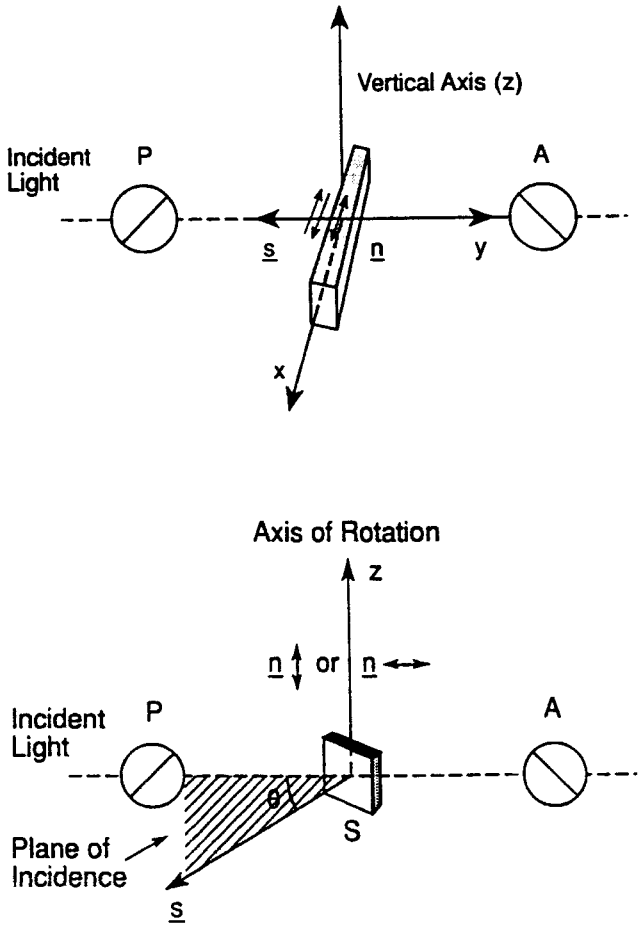

FIGURE 2 Schematic description of the experimental setup: (top) translation of a wedge sample, (bottom) Rotation of a plane parallel crystal.

where m_i is an integer. From two successive minima, say i and j, which obey $\delta_{ij} = |\delta_i - \delta_j| = |j - i|\ \lambda = |n_e - n_o|\ \tan\alpha\ |x_j - x_i|$, one can extract an estimate for the birefringence $|n_e - n_o|$ knowing the distance between the correponding displacements $|x_j - x_i|$ and the wedge angle α. The analysis of the data for this method is straightforward and provides an accurate measure of the birefringence $|n_e - n_o|$.

Method 2: Monitoring the incidence angle

In this method, the light path in the crystal is varied as the angle of incidence is monitored when a flat plane parallel crystal is rotated with

respect to the incident beam: $d' = d'(\theta')$. δ is given by Eqs. (5) and (7) for the geometries 1 and 2, respectively. A scan of the transmitted intensity as function of the angle of incidence θ provides an oscillating function. The minima occur at values of θ_i for which δ is an integer multiple of λ. For instance,

$$\delta i = m_i\lambda = d\left[1 - \left(\frac{\sin\theta_i}{\langle n_s\rangle}\right)^2\right]^{-\nu}(n_e - n_o) \qquad (15)$$

where $\nu = -1/2$ and $1/2$ for the geometries 1 and 2 respectively, and the order of the minimum m_i depends on the geometry: $m_i = m_i(\nu)$. In either case, for two successive minima i and j, such that $j = i+1$, δ obeys: $\delta_{ij} = |\delta_i - \delta_j| = \lambda$. A fit for the minima in the intensity curve I vs θ_i is required if accurate values for the refractive indices are needed (see below). However, the two geometries can provide values for the birefringence $|n_e - n_o|$, if approximate analytical expressions for δ (Eqs. (5) and (7)) are used and if $\langle n_s(\theta_i)\rangle$ and $\langle n_s\rangle$ are replaced by the constant $\bar{n}$.

Remark: Conoscopy

Monitoring the physical thickness d' (hence δ) may also be achieved if a sample is examined between crossed polars in highly convergent light beam.[1-3,9] The optical properties of the crystal are observed simultaneously at many propagation angles in the medium. When the transmitted beam is brought to interference in the focal plane of a lens, each point in this plane corresponds to a direction of parallel rays entering and leaving the crystal. For each ray, the path difference δ is a function of the angle made by this ray on the cone of light. For a planar uniaxial medium ($\underline{n}$ laying in the sample plane) and small birefringence, together with the conditions outlined above , $\psi = \pi/2$ and $|\phi| = \pi/4$, the interference figure is a set of hyperbolic fringes centered around the cone axis if $\underline{n}$ is orthogonal to the microscope optic axis.[1,2] Scanning the corresponding values of θ' on the cone of light and within the focal plane reveals oscillations of the intensity, as predicted by Eqs. (1) and (15).

Combining the use of the two methods for the same materials allows an accurate measurement for the individual refractive indices. From the wedge sample method, a value for $|n_e - n_o|$ is obtained; it is

afterwards used to fit the experimental data for geometry 1 in the first method. However, a numerical fit for the first method and the geometry 1 can provide values for the individual refractive indices if a reasonable estimate of $|n_e - n_o|$ is used and if d is known.

Materials

The materials used for the present study were conventional uniaxial quartz and dihydrogene potassium phosphate, KDP, crystals and a nematic lyotropic liquid crystal polymer system. For quartz, a uniaxial flat slab with 4190 ± 2 μ thickness and a wedge sample with an angle α ◻ 3 ± 0.02° were used for the present measurements. However, only a flat KDP crystal with 3968 ± 2 μ thickness was used. The optical axis $\underline{n}$ is kept laying within the sample plane for the two cases (Fig. 2). These crystals were provided by Cleveland Crystals Inc. Poly(p-phenylene benzobisthiazole), PBT, provided by SRI International through the courtesy of Dr. J. F. Wolfe and dissolved in methane sulfonic acid (MSA) was used as liquid crystal. The synthesis procedures, materials identification and solutions prepaparation are described elsewhere.[10-13] We simply recall the monodomain preparation and the experimental check for the orientation quality. We used PBT macromolecules with molecular weight M = 34,000, which corresponds to an average rod length of 160 nm, an index of polymerization of 320, and an aspect ratio of L/D ≈ 300 (where L stands for the rod length and D is the nominal diameter).[10-12] For the present study, only nematic solutions with a volume fraction ϕ beyond the critical value ϕ^* for the onset of the liquid crystal phase were used ($\phi^* \simeq 0.03$).[10-12]

Liquid crystal monodomains were obtained using good optical quality ($\lambda/4$ flatness) flat rectangular cells of 375 μ thickness and wedge cells with α = 0.95 ± 0.01°, provided by Hellma Cells Inc. Nematic monodomains were prepared as follows. The solution was extruded into the sample through a luer joint. Good quality and stable monodomains, useful for optic purposes, are obtained by applying a strong magnetic field (H ≈ 4 Tesla) to freshly prepared samples for several hours, with $\underline{H}$ parallel to the sample walls and to the flow direction. The alignment quality of the monodomains subsequently obtained was checked by looking at the conoscopic figures provided by these samples.[9]

Experimental arrangements

We used cw and pulsed light sources. The signals at λ = 514 nm and λ = 633 nm were provided by a tunable Ar^+ and a He–Ne lasers, respectively. The other visible wavelengths were obtained via second harmonic generation (SHG) from radiation in the near infrared (I.R.) spectrum and using a suitable crystal (Quartz or KDP for instance): $\lambda(2\omega)$ = 532 nm from $\lambda(\omega)$ = 1064 nm and $\lambda(2\omega)$ = 771 nm from $\lambda(\omega)$ = 1542 nm, respectively. An Nd:YAG pulsed source provides an intense nanosecond pulse at λ = 1,064 nm, and a Raman shifter, pumped with the incident YAG signal provides a pulsed signal at λ = 1,542 nm for methane gas (Stokes component).[7] The radiation at λ = 564 nm is also a Stokes component generated from methane when pumped with the fundamental signal at λ = 1064 nm (see above).[7]

The cw signal is detected using a photodiode, whereas the pulsed signal is detected using a photomultiplier tube, then digitized through the use of an ADC (LeCroy Inc.) system. A Nicol prism (CVI Laser Corp.) and a polarizing film were used to define the incoming polarization (P) and the outgoing polarization (A), respectively. Besides these elements, a visible bandpass filter, placed before the sample, selects the signal at 2ω after the harmonic source or the visible Stokes component (λ = 546 nm) after the Raman cell, and eliminates the fundamental I.R. beam. In addition, interference filters at the desired wavelength (see table I and II) were placed before the detector.

RESULTS AND DISCUSSION

Typical intensity curves for either method, the wedge crystal or the plane parallel slab (quartz, KDP, and PBT monodomain) are shown in Fig. 3. The coordinates represent the intensity I vs. translation distance x for wedge samples (Fig. 3a) and I vs. rotation angle θ for flat samples (Fig. 3b). Continuous lines are for cw radiations, whereas each point in the dotted graphs corresponds to a value of θ (or x) and an average over 10 shots for the pulsed radiation. An oscillating function I = I(θ or x), is easily observed as predicted by Eq. (1). The minima locations as well as their number, for a given rotation or translation intervals, depend on the geometry (n parallel or perpendicular to the plane of incidence), the wavelength λ, the sample

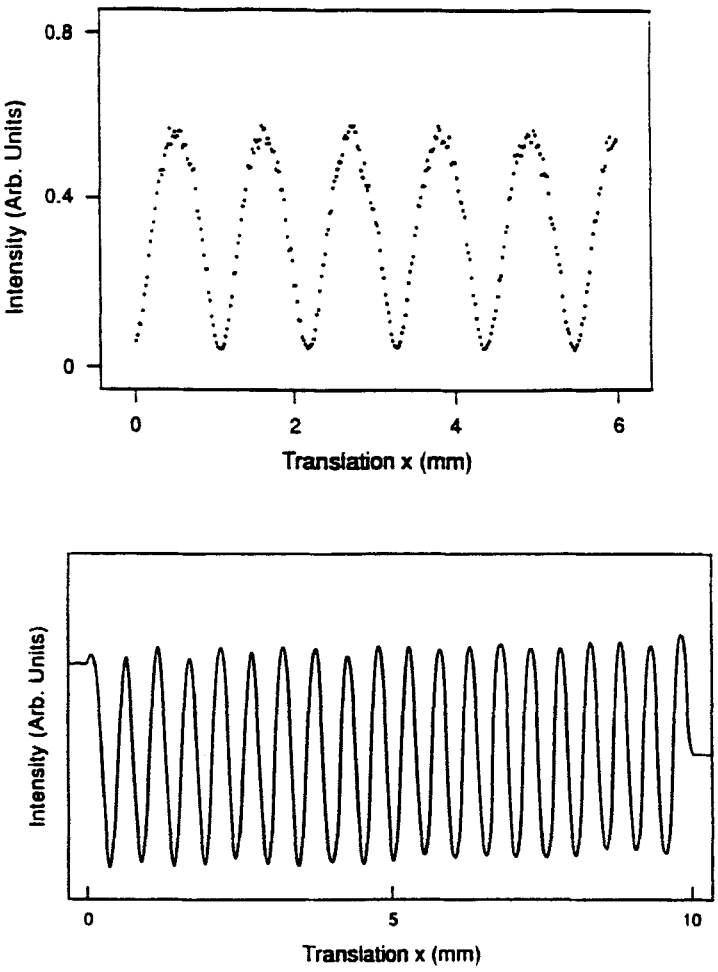

FIGURE 3a Plots of the intensity I vs. x for wedge samples: (top) wedged quatrz crystal (α = 3°) at λ = 532 nm; (bottom) wedged PBT monodomain (α = 0.95° and ϕ = 0.055) at λ = 633 nm.

thickness d for a flat sample or the wedge angle for a wedged crystal, and the medium birefringence.

Values for the birefringence $|n_e - n_o|$, using the wedged crystals, together with those using the "approximate" analysis (Eq. (5) for δ) and $\langle n_s \rangle = \bar{n}$ to fit the minima in I vs. θ curves for Method 2 and geometry 1, are reported in Table I for the different wavelengths and materials we used. It is important to notice the very good agreement between the values of $|n_e - n_o|$ measured using the two methods within the approximations introduced above, and those reported in the literature for the quartz and KDP reference.[6] In addition, the values

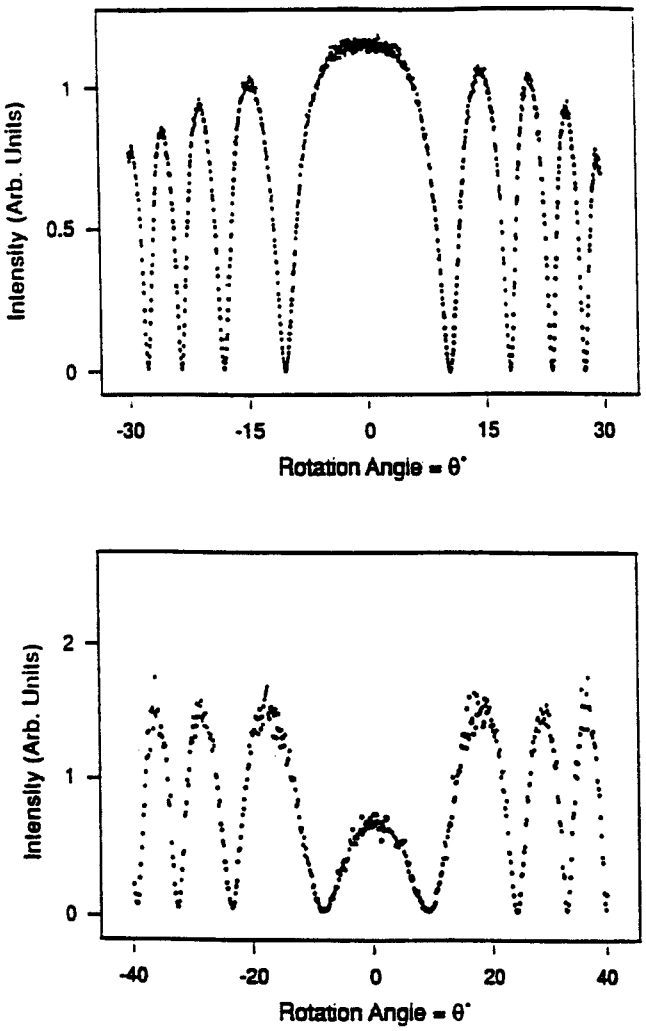

FIGURE 3b plots of I vs. θ for rotating plane parallel samples at λ = 532 nm: (top) plane parallel quartz (d = 4190 μ); (bottom) flat planar monodomain of PBT (d = 375 μ and ϕ = 0.055).

reached for all materials using the approximate fit for the Method 2 and the wedge case are also in good agreement. These agreements prove the success of the approximations made for the estimation of the birefringence (see above). The use of the birefringence values extracted above to fit numerically the data for the plane parallel crystal provides accurate values for the individual refractive indices. In fact, the refractive indices can be obtained using only the plane parallel crystal case as long as the sample thickness d is known, by using the full expression for $\langle n_s \rangle$ in Eq. (5) to fit the experimental data in the final analysis for this case, and starting from an estimate

TABLE I: Birefringence $|n_e - n_o|$.

	wedge method		approximate analysis, geom. 1, $\phi = \pi/4$ and $\psi = \pi/2$		
λ(nm)	Quartz $\alpha = 3^\circ$	PBT* $\alpha = 0.95^\circ$	Quartz $d = 4190\mu$	KDP $d = 3968\mu$	PBT* $d = 375\mu$
514	–	–	–	–	0.121
532	0.00927	–	0.00925	0.0425	0.1115
564	0.00920	–	–	–	0.0910
633	0.00915	0.074	0.0091	0.0408	0.078
771	0.00894	0.0615	0.0089	–	0.061

*PBT monodomain with $\phi = 0.055$

of the birefringence from the approximate analysis from method 2. This procedure was helpful if a wedge crystal for the compound was not available. Table II summarizes the values for n_e, n_o, and the corresponding $|n_e - n_o|$, hereby measured, using the procedure (numerical fit) described above.

The values measured for the conventional uniaxial crystals (quartz and KDP) using the present technique are in very good agreement with those reported in the literature.[6,14] In addition, the present set of data provide values at wavelengths that have not been scanned previously (Ref. 6 and 14). For the PBT monodomain, the birefringence measured is larger than what has been reported for other lyotropic polymer liquid crystals. However, these materials have smaller aspect ratio and complex helical structures are often involved in the chain as, for instance, are the cases for TMV and PBLG.[20] The dispersion is also more pronounced than that has been reported for other low molecular weight liquid crystals.[17-19] The data for the quartz and PBT monodomain used in the present study fit successfully a classical empirical expression based on the Lorentz oscillator for each component of the refractive indices,[1-3]

TABLE II: Individual refractive indices from the numerical fit for method 2 using the birefringence from the previous case (TABLE I).

	Quartz d = 4190μ			KDP d = 3968μ		
λ(nm)	n_o	n_e	$(n_e - n_o)$	n_o	n_e	$(n_e - n_o)$
514	-	-	-	-	-	-
532	1.54678	1.55605	0.00927	1.51243	1.47060	-0.04183
564	-	-	-	-	-	-
633	1.54330	1.55244	0.00914	1.50770	1.46678	-0.04092
771	1.53830	1.54731	0.00901	-	-	-

PBT Monodomain
ϕ = 0.055, d = 375 μ

λ(nm)	n_o	n_e	$(n_e - n_o)$
514	1.5270	1.6480	0.1210
532	1.5158	1.6318	0.1160
564	1.50619	1.59689	0.0907
633	1.4990	1.5770	0.0780
771	1.48004	1.54264	0.0626

$$R = \frac{n^2 - 1}{n^2 + 2} = \frac{K\lambda_m^{-2}}{\lambda_m^{-2} - \lambda^{-2}} \qquad (16)$$

where $K\lambda_m^{-2}$ is an average oscillator strength (Fig. 4). The agreement, which is observed for all wavelengths in the visible range, completes our previous study where few wavelengths were scanned but which

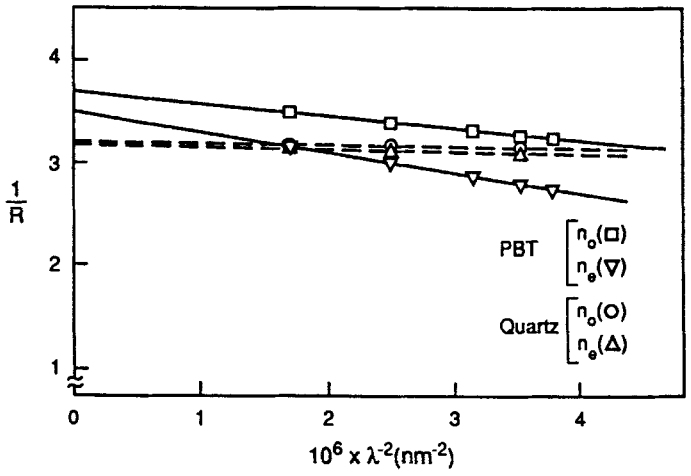

FIGURE 4 plot of 1/R vs. $1/\lambda^2$ for the extraordinary and ordinary refractive indices of the quartz crystal and PBT monodomain studied.

included near I.R. wavelengths.[9] For the PBT monodomain, a single constant K is measured for both cases ordinary and extraordinary, whereas two different values for λ_m were extracted: $\lambda_m)_e \simeq 250$ nm, and $\lambda_m)_o \simeq 200$ nm. The difference is associated with the dichroism of the absorption in the UV region. However, the present values for the oscillator strength, $(K\lambda_m^{-2})_e < (K\lambda_m^{-2})_o$, suggest that an inversion in the dichroism for the lower UV region of the spectrum emerges, as opposed to the case for the absorption peak in the visible region around $\lambda = 436$ nm. For this peak, the absorption parallel to the rod axis (extraordinary) is larger than the one normal to that axis.[10]

The present set of data for the refractive indices and their dispersion are also very useful for analyzing nonlinear optical (NLO) data using harmonic generation technique.[4,5,15,16] They intervene in the estimate of the coherence length, defined as $\ell_{c,i} = \lambda_\omega / |n_{i\omega} - n_\omega|$ with i = 2 or 3 for second and third harmonic generation (SHG and THG), respectively, of the material as well as its anisotropy (ω designates the frequency of the incident radiation).[4] They also intervene in the estimate of the susceptibility coefficient as well as its anisotropy for uniaxial media, since the harmonic intensity provided by the experiment is directly related to the ratio $\{\chi^{(i)}/|n_{i\omega}^2 - n_\omega^2|\}^2$, i = 2 or 3 (see above). The anisotropy in the dispersion for the PBT *monodomain* provided an insight into the understanding of the NLO

data obtained from THG measurements. This comparison is discussed in detail in a forthcoming publication.[16]

The present technique offers an independent method to measure the individual refractive indices and/or the birefringence of uniaxial materials, and may also be used to study biaxial materials.[21]

CONCLUSION

Anisotropy of the refractive index and its dispersion for radiation in the visible region of the optical spectrum were presented for uniaxial media. The technique uses the optical anisotropy of the nematic (or any uniaxial medium) to generate an interference between the ordinary and extraordinary waves in the crystal. We discussed the implications of the present set of data on the third harmonic generated interference patterns provided by these materials. The measurement of the dispersion, mostly its strong anisotropy, provided a better insight into the understanding of the THG Maker Fringe Patterns for these solutions and the correlation between the geometry(ies) and the patterns obtained.[15,16]

Acknowledgments

We thank the Air Force Office of Scientific Research, AFOSR, for partial support. We benefited from fruitful discussions with professor G. D. Patterson. We also thank D. Fishman and K. Kauffmann for carefully reading the manuscript.

REFERENCES

1. "*Oeuvres Completes d'Auguste Fresnel*", Published by De Senarmont, H., Verdet, E., Fresnel, L., **VI**, Imprimerie Imperiale, Paris (1866).
2. Born, M., Wolfe, E., *"Principles of Optics"*, Pergamon Press, Oxford (U.K.), sixth Edition (1980).
3. - De Jeu, W. H. *"Physical Properties of Liquid Crystalline Materials"*, Gordon and Breach Science Publishers, New York (1980).
   - Haller, I., Huggins, H. A., and Freiser, M. J., *Mol. Cryst. Liq. Cryst.*, **16**, 53 (1972).
4. Kurtz, S. K., in *"Quantum Electronics"*, Ed. by Rabin, H., and Tang, C. L., **VI**, Part A, Academic Press, N.Y. (1975) Ch. 3.
5. Shen, Y. R., *"The Principles of Nonlinear Optics"*, J. Wiley, N.Y. (1984).
6. Yariv, A. *"Optical Electronics"*, Holt, Rinehart and Winston,

3rd. Edition, New York (1985).
7. Kajzar, F., Messier, J., *Phys. Rev. A*, 32, 2353 (1985).
8. "*Nonlinear Optical Properties of Organic Molecules and Crystals*", Edited by Chemla, D. S., Zyss, J., V1 & V2, Academic Press, N.Y. (1987).
9. Mattoussi, H., Srinivasarao, M., Kaatz P. G., and Berry, G. C., *Macromolecules*, in press.
10. a. Venkatraman, S., Ph.D. dissertation, Carnegie Mellon University (1981).
    b. Srinivasarao, M., Ph.D. dissertation, Carnegie Mellon University (1990).
11. Wei-Berk, C., Berry, G. C., *J. App. Polym. Sci., Polym. Phys.* Ed., in press.
12. Lee, C. C., Chu, S. G., Berry, G. C., *J. Polym. Sci. Polym. Phys.* Ed., 21, 1573 (1983).
13. Metzger Cotts, P., Berry, G. C., *J. Polym. Sci. Polym. Phys.* Ed., 21, 1255 (1983).
14. Wolfe, W. L., in "*Handbook of Optics*", Optical Society of America, Ed. by Driscoll, W. G., and Vaughan, W., Mc Graw Hill (1978), Section 7.
15. Mattoussi, H., Berry, G. C., *ACS Polym. Preprints*, 32 (3), 690 (1991).
16. Mattoussi, H., Berry, G. C., to be submitted for publication.
17. Chang, R., *Mol. Cryst. Liq. Cryst.*, 30, 155 (1975).
18. Kuczynski, W., Stryta, B., *Mol. Cryst. Liq. Cryst.*, 31, 267 (1975).
19. Hanson, E. G., Shen, Y. R., *Mol. Cryst. Liq. Cryst.*, 36, 193 (1976).
20. Murthy, S. N., Knox, J. R., Samulski, E. T., *J. Chem. Phys.*, 65, 4835 (1976); Oldenbourg, R., Wen, X., Meyer, R. B., *Phys. Rev. Lett.*, 61, 1851 (1988).
21. Kerkoc, P., Zgonik, M., Sutter, K., Bosshard, C., Gunter, P., *J. Opt. Soc. Am.* B7, 313 (1991).